

## Simulations of Filled Polymers on Multiple Length Scales

**Francis W. Starr and Sharon C. Glotzer**

Polymers Division and Center for Theoretical and Computational Materials Science,  
National Institute of Standards and Technology,  
Gaithersburg, MD 20899

### ABSTRACT

We present simulation results of the effect of nanoscopic and micron-sized fillers on the structure, dynamics and mechanical properties of polymer melts and blends. At the smallest length scales, we use molecular dynamics simulations to study the effect of a single nano-filler on the structure and dynamics of the surrounding melt. We find a tendency for polymer chains to be elongated and flattened near the filler surface. Additionally, the simulations show that the dynamics of the polymers can be dramatically altered by the choice of polymer-filler interactions. We use time-dependent Ginzburg-Landau simulations to model the mesoscale phase-separation of an ultra-thin blend film in the presence of an immobilized filler particle. These simulations show the influence of filler particles on the mesoscale blend structure when one component of the blend preferentially wets the filler. Finally, we present some preliminary finite element calculations used to predict the effect of mesoscale structure on macroscopic ultra-thin film mechanical properties.

### INTRODUCTION

Revolutionary advances in the design and fabrication of new materials that are lightweight and high strength will come from advances in the fundamental understanding of nanocomposites, in which nanoscopic fillers (“nanofillers”) are dispersed on nanometer scales within the polymer matrix [1,2,3]. Already, major enhancements in mechanical, rheological, dielectric, optical, and other properties of polymer materials have been achieved by adding fillers such as carbon black, talc, silica, and other inexpensive, inorganic materials. Nanofillers such as nanotubes, silica beads and cages, and clays, offer phenomenal advantages over these more traditional fillers because greater property improvement is achieved with far less material (see Figure 1 for examples of filler and nanofiller geometries). For example, adding 1% by weight of ultra-fine, synthetic mica (30-nm diameter disks) to nylon gives super-tough nylon, while adding the same amount of traditional mica (micron-sized talc) gives only a slight improvement in toughness over the unfilled polymer.

The growing ability to design customized nanofillers of arbitrary shape and functionality provides an enormous variety of possible property modifications by introducing specific heterogeneity at the nanoscale [2,4,5]. However, little is known about the specific influence of nanofillers on the polymers surrounding them, and thus the development of highly designed, nanostructured materials for specific applications is currently limited. Future breakthroughs in the development of organic/inorganic hybrid nanocomposites will be possible by manipulating the inorganic phase on nanometer scales in order to achieve specific properties. Achieving such capability will require insight on many length scales, ranging from the interfacial interactions on molecular scales, to the ordering and assembly of inorganic phases on lengths scales from several tens of nanometers to tens of microns, to the manifestation of bulk material properties on

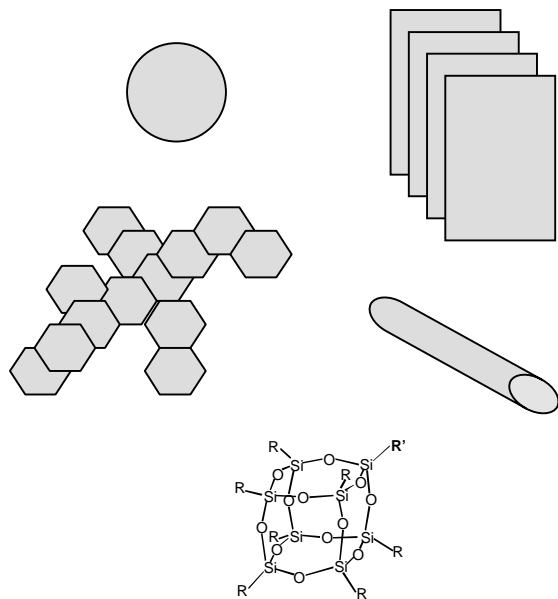


**Figure 1.** Examples of filler and nanofiller geometries. Clockwise from upper left: (a) spherical (e.g. colloidal silica); (b) sheets (e.g. clays); (c) rods, tubes, and fibers (e.g. carbon nanotubes); (d) cubes (e.g. cubic silsesquioxanes); and (e) fractal (e.g. fumed or precipitated silica, carbon black, where the primary particle may be polyhedral, as for carbon black, or spherical, as for fumed silica).

macroscopic scales. Computer simulation will play an essential role in materials discovery and optimization, and in interpreting and guiding experiments to probe and manipulate these materials on molecular scales.

Filled polymers and nanocomposites pose a particular challenge to computer simulation, because they possess a hierarchy of length and time scales resulting not just from the polymer itself, but also from the structure of the filler or nanofiller. As a result, in modeling filled polymers, in principle one must capture phenomena on length scales that span typically 5-6 orders of magnitude, and time scales that can span a dozen orders of magnitude.

As an example, consider carbon black (figure 2). At the smallest scale, carbon black is made of small, nearly graphitic, faceted particles that can range from 4 to several hundred nanometers across, depending on how they are produced [1]. During synthesis (while still molten), these so-called “primary particles” permanently fuse together into random structures, or “aggregates”, which make up the smallest dispersible unit. These aggregates can in turn physically associate into larger and larger agglomerates, which are not permanent and can be broken up on shearing. If we consider filled polymer blends, the immiscibility of the blend provides even more structure to the material.

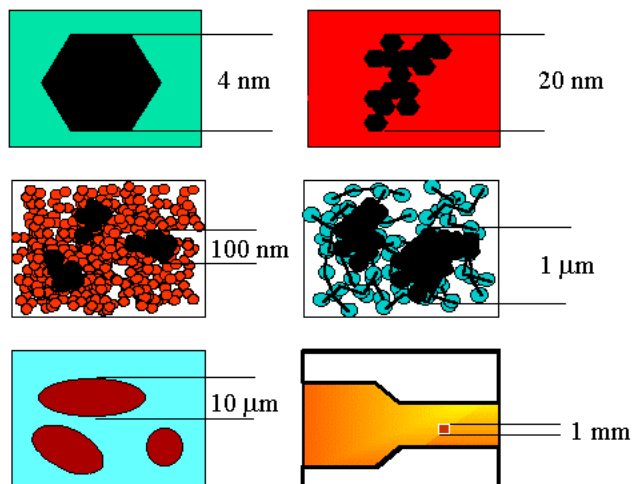


**Figure 2.** Example of the range of length scales on which phenomena must be modeled for carbon black filled polymers, ranging from the length scale of (a) the smallest primary particle; (b) an aggregate, the smallest dispersible unit; (c) and (d) agglomerates; (e) phase-separated domains; and (f) during flow (figure from [12]).

In order to bridge these disparate length and time scales, we present three different simulation studies of filled and nanofilled polymers, each aimed at extracting fundamental information on a different scale. Each study involves a different simulation method appropriate for the particular phenomena of interest. In the first study, we use molecular dynamics (MD) simulations [6] to explore the effect of a single nanoscopic, model filler particle on the structure, dynamics, and glass transition temperature of a model polymer melt [7]. In the second study, we use time-dependent Ginzburg-Landau (TDGL) methods [8] to study the effect of model nanometer to micron-sized fillers on the mesoscale structure of phase-separating polymer blends [9]. In the third study, we use the finite element method [10] in a preliminary study to probe the effect of fillers on the mechanical properties of filled blend microstructures [11]. Although the studies are performed independently, we outline ways in which information gleaned from one simulation is used in another in order to bridge the length scales necessary to link molecular phenomena to macroscopic properties.

## MOLECULAR SIMULATIONS

Molecular dynamics simulations provide an ideal opportunity for direct insight into the effects of fillers on polymer structure and dynamics in the vicinity of the polymer-filler interface. As an example, we present results of an MD study of a polymer melt containing a single nanoscopic filler particle [7]. We can trivially adjust the interaction parameters between the filler and the surrounding polymer melt; the explicit control of the interactions helps to clarify which changes in the melt properties result from the type of interaction, and which properties change as a result of the steric hindrance introduced by the filler particle. This relatively simple single filler model provides an initial framework in which to interpret experiments on filled polymers [13-16], and also possibly polymer thin films [17-26], which report both increases and decreases of the glass transition temperature  $T_g$ , depending on the details of the system studied. In the case of filled polymers, future studies should consider the complicated geometrical effects that arise from the presence of multiple filler particles.

Our findings are based on extensive molecular dynamics simulations of a single nanoscopic filler particle surrounded by a dense polymer melt of 20-mer chains (figure 3). We use a “bead-spring” model for the polymers in which all monomers interact via a Lennard Jones (LJ) potential. Nearest-neighbor monomers along the same chain are bound together via a FENE anharmonic spring potential [27]. This simple polymer model has been studied in detail, and is known to be a good glass forming system, due to the imposed incompatibility of the preferred FENE bond distance and the LJ potential minimum [28,29].

Our model filler has several general features typical of a primary carbon black particle, as well as some newer nanofillers [1]; it is highly faceted, but nearly spherical, and has facets with a size of about 10 nm. Specifically, the filler particle is icosahedral and has a facet size roughly equal to the end-to-end distance of the surrounding polymers. There are 356 force sites associated with the filler that interact with each other via a LJ potential with twice the strength of the polymer-polymer interactions.

We consider two possible forms for the interaction between filler sites and monomers to determine which properties are a result of the steric constraints imposed by the filler, and which properties are affected by polymer-filler attraction. The system is comprised of a melt surrounding a single filler with either (i) an excluded volume interaction only or (ii) excluded volume plus attractive interactions – a LJ interaction. The excluded volume interaction is

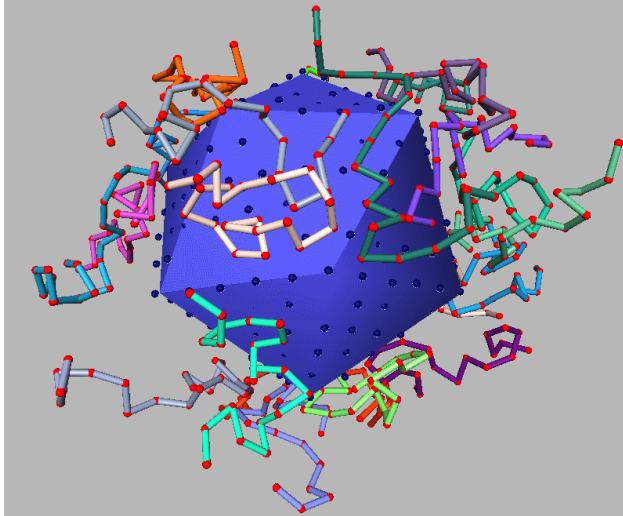


**Figure 3.** The model filler particle is the central blue object. A selection of the polymers from the whole system that are near the surface are shown.

modeled by dropping the attractive  $r^6$  term in the LJ potential. The simulation is performed in a cubic cell with periodic boundary conditions and the size of the cell is chosen such that the density  $\rho$  far from the filler particle is nearly constant. Since we wish to know how the filler changes the melt properties relative to the pure melt we also simulate an unfilled melt at density  $\rho = 1.0$ .

We first consider changes in the polymer structure caused by the nanofiller. As in the case of polymers near a flat surface such as a wall [20,21], the density profile of the monomers has a well-defined layer structure (figure 4). In the attractive case, we see a pronounced enhancement in the polymer density in the first layer, which we expect due to the relatively strong filler-monomer attraction; these density oscillations persist over a distance of roughly four monomers. The density profile depends weakly on temperature, becoming better defined as  $T$  decreases. It is somewhat surprising, in the case of excluded volume interactions, that there is an enhancement in the density in the first layer. However, notice that the location of the first layer is “pushed out” slightly, in comparison to the attractive filler case. The position of this peak increases with decreasing  $T$ , since the monomers have less kinetic energy, limiting the distance of closest approach.

The changes in the density profile must also be accompanied by some change in the local packing of the polymers. By focusing on the dependence of  $R_g$  on the distance from the filler surface (figure 5), we find a change in the overall polymer structure near the surface.  $R_g^2$

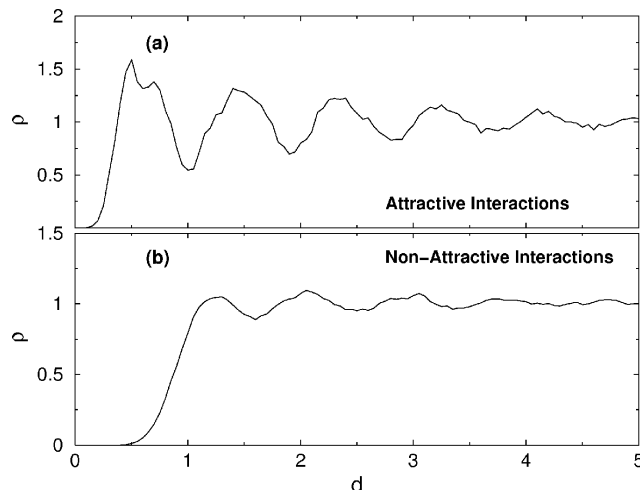


**Figure 4.** The local density of monomers as a function of the distance  $d$  from the filler surface. Formally, we define  $d$  as the difference between the radial position of a monomer and the radius of the inscribed sphere

$$r_{i\cos} = \frac{1}{12} (42 + 18\sqrt{5})^{1/2} L \text{ of the icosahedral filler particle.}$$

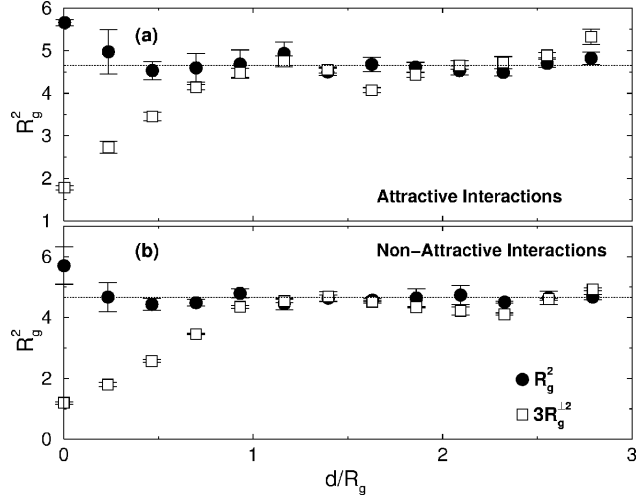


**Figure 5.** Radius of gyration, and its perpendicular component as a function of the distance of the center of mass of the polymer chain from the filler surface, as defined in Figure 4.

increases by 50% on approaching the filler surface in both cases, and the perpendicular component  $(R_g^\perp)^2$  decreases by slightly more than a factor of 2. This indicates that the polymers become slightly elongated near the surface, and flatten significantly. The independence of the chain structure on the interaction suggests that the altered shape of the polymers is primarily due to geometric constraints of packing the chains close to the surface. Interactions seem to play a far more important role in changes of the dynamics of the system, as we see in the following.

To quantify the effect of the filler on dynamic properties, we calculate the intermediate scattering function

$$F(q, t) \equiv \frac{1}{NS(q)} \sum_{j,k=1}^N e^{-iq \cdot (r_j(t) - r_k(0))}, \quad (1)$$

which measures the decay of density fluctuations in the system, and is immediately accessible to neutron scattering experiments and other techniques [30]. Here  $N$  is the total number of monomers. We define the relaxation time  $\tau$  by  $F(q_0, \tau) = 0.2$ , where  $q_0$  is the wave-vector corresponding to the main peak in the static structure factor  $S(q)$ . Relative to the pure melt, we find that  $\tau$  increases in the filled system with attractive interactions, but decreases slightly for the filled system with only excluded volume interactions; in other words, the attractive interactions appears to slow the dynamics relative to the pure melt, while the excluded volume (non-attractive) interactions shows a slight enhancement of the dynamics.

From an experimental standpoint, the change in dynamics is most frequently indicated by a shift in the overall glass transition in the system. Based on our observations of  $\tau$ , we would expect that the  $T_g$  of the attractive system would be somewhat larger than the pure melt, while the excluded volume system would exhibit a suppressed  $T_g$ . We check if these expectations are correct by estimating  $T_g$  using the Vogel-Fulcher-Tamman-Hesse form [31]

$$\tau = \tau_0 e^{\frac{A}{T - T_0}}, \quad (2)$$

where the parameter  $T_0$  is known to be close to the experimentally measured  $T_g$ , and also exhibits the same changes found in  $T_g$ . For the pure system, we find  $T_0 = 0.167$ . Consistent with our expectations, we find that  $T_0$  increases ( $T_0 = 0.184$ ) for the attractive filler, and decreases ( $T_0 = 0.156$ ) for the non-attractive filler. The fact that  $T_0$  shifts in opposite directions for attractive versus purely excluded volume interactions demonstrates the importance of the surface interactions. We also estimate  $T_0$  for systems with a smaller number of polymers, and hence greater surface-to-volume ratios, to better understand the importance of surface interactions.

Figure 6(a) shows that the shifts of  $T_0$  as a function of the mass fraction  $\phi$  of the filler become increasingly pronounced with increasing  $\phi$ .

We can explain these more pronounced shifts by focusing on the influence of the filler on the local dynamics of the monomers. We do this by calculating the relaxation of the self (incoherent) part  $F_{\text{self}}(q,t)$  of  $F(q,t)$  as a function of the monomer distance from the filler. We split  $F_{\text{self}}(q,t)$  into the contribution from the separate layers previously observed in figure 4. For the attractive system (figure 6(b)), the relaxation of the layers closest to the filler is slowest, consistent with the system dynamics being slowed by the attraction to the filler. As the number of polymers in the system is reduced, the slow surface dynamics become increasingly important, and so we find an increased shift of  $T_0$ . Conversely, for the non-attractive system (not shown), we find that the relaxation of inner layer monomers is significantly enhanced compared to the bulk, consistent with the observed decrease of  $T_0$ .

Our results strongly suggest that interactions play a key role in controlling  $T_g$  and the local dynamics of filled polymers [32]. We expect the role of interactions to be largely the same when many filler particles are present in the melt, but there will be additional effects on dynamic properties due to the more complex geometrical constraints. These dynamic changes are likely also reflected in the thermodynamic properties, most notably in the configurational entropy [35,36], long used to rationalize dynamic properties, and recently tested directly in simulations [37,38,39]. Additionally, we point out that our results show striking similarity with those obtained for ultra-thin polymer films, which suggests that the underlying physics in these systems is very similar, and is dominated by surface interactions [40,41]. Hence the pre-existing knowledge of thin-films may be useful for understanding and developing filled polymer materials, as discussed in ref. [7].

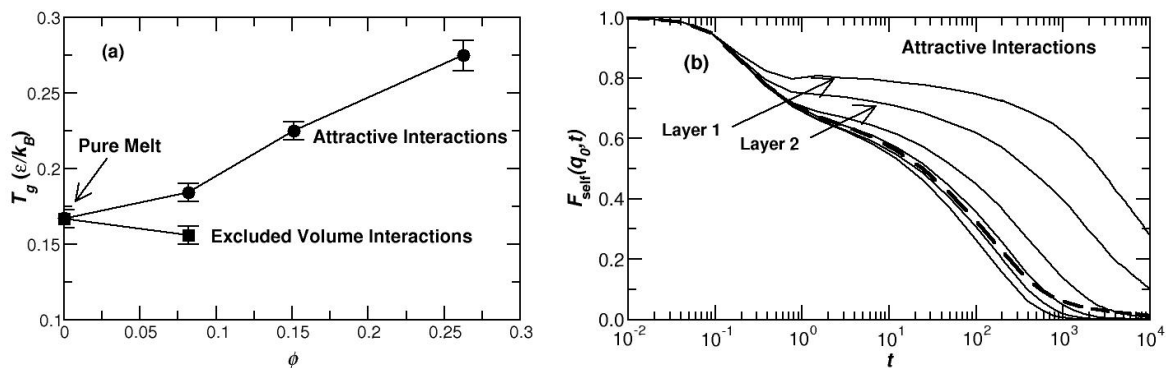


**Figure 6.** (a) Effect of the mass fraction  $\phi$  of filler on the estimated  $T_g$ . Increasing  $\phi$  increases the surface-to-volume ratio, so that surface interactions become more important.

(b) Relaxation of the self-part of the intermediate scattering function decomposed into the contribution of each layer of monomers around the filler, as in Figure 4. The dotted line is the system average. The surface monomers exhibit the slowest dynamics in the case of the attractive filler, explaining the increased  $T_g$  shift as  $\phi$  increases. In the case of the non-attractive filler (shown in ref. [7]), the surface monomers exhibit the fastest relaxation.

## MESOSCALE SIMULATIONS

The molecular dynamics results of the previous section can be used to design mesoscale simulations of filled polymer blends. Polymer blends, which are mixtures of two or more types of polymers, are generally immiscible, and will phase separate by a process called spinodal decomposition when the temperature, pressure, and blend composition are such that the blend is thermodynamically unstable. During this non-equilibrium process, domains rich in polymer A or polymer B (in the case of a binary blend) will form and coarsen in a self-similar way, eventually forming co-existing, macroscopic phases. In many instances, the phase-separating patterns can be trapped in the material by quenching the blend below  $T_g$  before the separation process is complete. When fillers are present in the blend, a preferential attraction of one of the polymers to the filler can break the symmetry of the spinodal decomposition process, producing novel mesoscale patterns and possibly even modifying domain growth laws.

A popular mesoscale method for simulating the structural evolution of phase-separation morphology in blends is the so-called time-dependent Ginzburg-Landau (TDGL) method. This method is based on the Cahn-Hilliard and Cahn-Hilliard-Cook (CHC) models [42,43], and falls under the more general category of phase-field and reaction-diffusion models. In this approach, a free energy functional  $F[\phi]$ , which depends on a conserved local spatiotemporal concentration field  $\phi(\mathbf{x}, t)$  given by, e.g., the local fraction of polymer A, is minimized to simulate a temperature quench from the miscible region of the phase diagram to the immiscible region where the blend is thermodynamically unstable. In this way, the resulting time-dependent structural evolution of the blend as it phase separates by spinodal decomposition can be investigated by solving the CHC/TDGL equation for the time dependence of the local blend concentration  $\phi$ ,

$$\frac{\partial \phi(\mathbf{x}, t)}{\partial t} = \nabla \cdot M \nabla \frac{\partial F[\phi]}{\partial \phi(\mathbf{x})} + \xi(\mathbf{x}, t). \quad (3)$$

Here  $M$  is the mobility, which in general may depend on  $\phi(\mathbf{x}, t)$ , and  $\xi$  is a thermal noise term.  $F[\phi]$  consists of a bulk free energy term (e.g., the Flory-Huggins expression, or a Landau expression), and at minimum a square gradient term. A pedagogical discussion of this method and its application to blends and filled blends can be found in the refs. [8,9].

Numerous studies of blend phase separation under various conditions have been performed using this approach, including reactive blend phase separation [44-48], phase separation of liquid crystal/polymer blends [49], phase separation under shear [50,51], phase separation of block copolymers [52,53], and phase separation on patterned surfaces [54].

The TDGL method has recently been applied to the study of phase separation in ultra-thin, filled blend films [9,51,55,56]. Ultra-thin blend films are thin enough ( $\ll 100$  nm) to suppress phase separation transverse to the solid substrate (“surface-directed spinodal decomposition”) so that phase separation occurs quasi-two-dimensionally in the plane of the film. A preferential attraction for one of the blend components by the filler can be modeled by adding a local surface interaction energy  $F_s[\phi]$  to  $F[\phi]$ , which is expressed as an integral over the surface of the particle. A minimal model of phase separation near boundaries is given in ref. [9] (and references therein) in which the surface interaction energy is given by

$$F_s[\phi] = \int_s d^{d-1}x [h\phi + \frac{1}{2}g\phi^2 + \dots], \quad (4)$$

subject to boundary conditions of zero flux and local equilibrium at the filler surface. Here, the coupling constant  $h$  in the leading term plays the role of a surface field that breaks the symmetry

between the two phases and attracts one of the blend components to the filler surface. The value of  $h$  can be related to the interaction energy  $\varepsilon_{mf}$  in the previous section. The coupling constant  $g$  in the second term is neutral regarding the phases, and results from the modification of the interaction energy due to chain connectivity [57,58] and the missing neighbors near the surface when the equation is solved on a grid [59,60]. The attractive interaction between filler and polymer A causes wetting of the filler by the polymer, analogous to the density enhancement shown in Figure 4(a), which breaks the symmetry of the spinodal decomposition process, producing novel patterns.

When the filler particles are immobile on the time scale of phase separation, transient “target” patterns (figure 7) are observed. As shown in figure 7, the observed “target” composition pattern is well developed at early times, but fragments as the “background” spinodal phase-separation pattern coarsens to a length scale larger than the filler particle. The scale of the phase-separation pattern in this simulation grows with the usual  $t^{1/3}$  power law over the time range indicated in the figure [7]. This growth law is independent of spatial dimension and is characteristic of the intermediate stage of phase separation in blends when hydrodynamic effects are not important. The extent to which the target pattern extends into the background spinodal pattern can be controlled through the quench depth, we depends on both the polymer molecular weight and the quench temperature.

Similar target patterns were observed via atomic force microscopy in a colloidal-silica-filled ultra-thin film blend of PS/PVME, in which the PS is preferentially attracted to the silica beads [61]. In the experiment, the filler was immobilized on the substrate supporting the film, and thus the conditions were very similar to those in the simulation. The patterns were trapped in the film by quenching below  $T_g$  before the spinodal decomposition process was completed.

The results shown here were obtained using a constant, composition- and spatially-independent mobility  $M$ , and represent a “minimal model” of the effect of fillers on phase separation morphology. To more accurately model the effect of filler interactions on the mesoscale structure of immiscible blends, we can use the results of the previous section in future studies to modify  $M$  so as to slow the polymer dynamics of the wetting phase, and speed up the dynamics of the non-wetting phase. This may have the effect of prolonging the lifetime of the target patterns, and/or increasing the distance over which they penetrate into the background

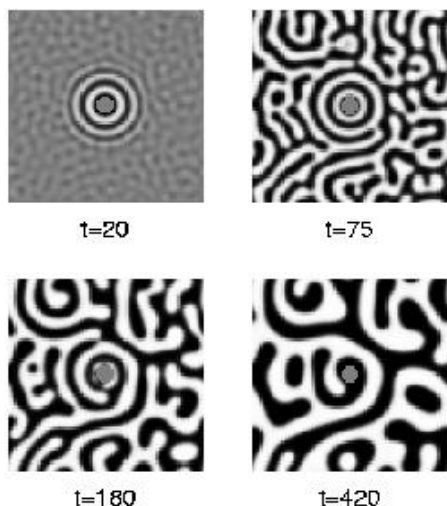


**Figure 7.** Simulation of the influence of a single isolated filler particle (central gray region in the figure) on polymer-blend phase separation, where the filler is immobile (from ref. [9]). We show the concentration field  $\phi$  at four different times following a quench to a two-phase region. Here black denotes the polymer-A rich phase, which wets the filler, and white denotes the polymer-B rich phase.

spinodal pattern. It would also be interesting to incorporate  $T$  dependence in the mobility in order to capture certain aspects of glass transition phenomenology, and compressibility to accurately model the spatial dependence of the density variation of the wetting phase. In the present studies, the filler particles were considered immobile on the time scale of phase separation in order to compare with ultra-thin film experiments, where silica beads were essentially attached to the surface; introducing filler mobility into the model may modify the mesoscale structure [55,56]. As shown in the next section, representative microstructures obtained from the TDGL/CHC approach can be used as input to finite element packages such as OOF to predict elastic properties, thereby bridging several key length scales relevant to filled polymers.

## MACROSCALE MECHANICAL PROPERTY SIMULATIONS

Fillers added to polymer blends can modify mechanical properties of the blend in several ways. First, the filler itself can impart additional strength and toughness through its own mechanical properties. Second, the filler can inhibit failure by blocking the propagation of cracks. Third, the modification of polymer structure near the filler surface that we observed in our MD simulations can alter mechanical properties. And because mechanical properties depend on material microstructure, fillers can alter, e.g., the blend modulus through the modification of microstructure as demonstrated in the previous section.

A new software tool developed at NIST, called OOF [62,63] facilitates the prediction of mechanical properties of materials by using real or simulated microstructures as input. OOF allows users to assign specific constitutive properties, such as modulus, etc., to the various parts of the microstructure, construct a finite element mesh to resolve the key features of the microstructure, and perform mechanical simulations using the finite element method. In this way, the effect of changes in microstructure on mechanical properties can be easily determined.

The current generation of OOF software assumes the behavior of the material is linear elastic (OOF was originally developed for ceramic materials, but is enjoying much broader application.) The next generation of the tool, OOF2, will allow incorporation of, e.g., nonlinear elasticity.

As one example of how OOF can be used for filled polymer blends, we have performed preliminary calculations of the elastic modulus of two critical composition blend microstructures (figure 8). The first microstructure is obtained from a simulation of the TDGL/CHC equation in the absence of fillers, and the second is obtained from the same simulation but with fillers included, as in Figure 7. Both simulations were stopped after the same number of time steps; in the absence of fillers, the blend microstructure coarsens to larger domain sizes. We assume both components are rubbery, and assume relative Young's moduli for the two phases of 10:1. We further assume the interfaces between the two phases to be sharp. We then apply a 10% longitudinal strain in the  $x$ -direction to both microstructures. If we neglect the additional modification of the mechanical properties due to the filler properties, and focus only on the effect of microstructure, we find that the bottom microstructure in Figure 8 has an elastic modulus roughly 18% smaller than the modulus of the top microstructure in Figure 8. The bright and dark features in the microstructures indicate regions of high and low local strain, respectively. As expected, the high strain regions correspond to the low modulus phase. Additional work is underway to extend this preliminary study, and will be reported elsewhere [64].

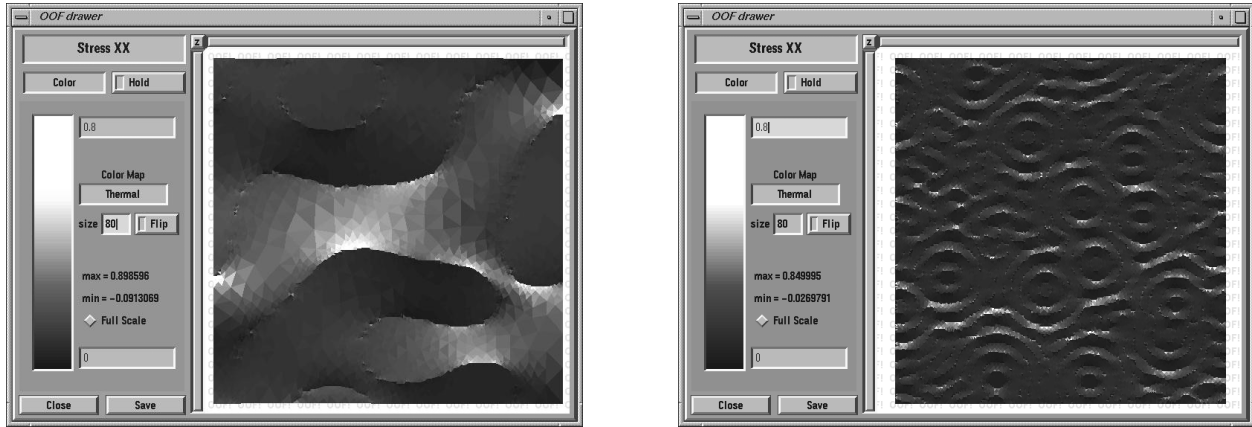


**Figure 8.** Example of OOF mechanical property calculations on two different blend microstructures resulting from phase separation in the absence of fillers (left) and presence of fillers (right). Color scheme: bright spots indicated regions of high local strain, and occur in the lower modulus phase [11].

## CONCLUSIONS

We have described three different simulation studies of filled and nanofilled polymers, each aimed at extracting fundamental information on different length and time scales. Each study involved a different simulation method appropriate for the particular phenomena of interest. In the first study, MD simulations were used to explore the effect of a single nanoscopic, model filler particle on the structure, dynamics, and glass transition temperature of a model polymer melt. In the second study, TDGL/CHC methods were used to study the effect of model nanometer to micron-sized fillers on the mesoscale structure of phase-separating polymer blends. In the third study, finite element methods were used to probe the effect of fillers on the mechanical properties of blend microstructures. Although the studies were performed “off-line”, we outlined ways in which information gleaned from one simulation can be used in another to bridge the length scales necessary to link molecular phenomena to macroscopic properties, depicted schematically in Figure 9.

The link between mesoscale structure and macroscale mechanical properties was accomplished by using the output of the TDGL/CHC simulations as input for the OOF

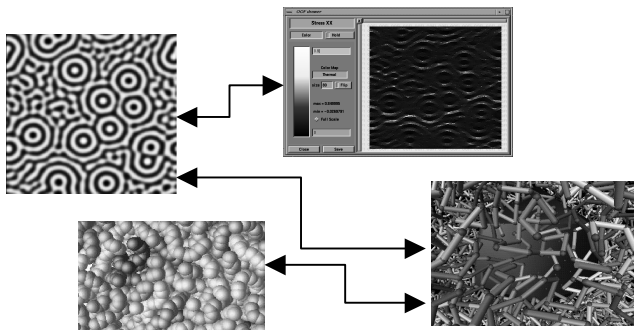


**Figure 9.** One possible paradigm for the integration of length scales in the simulation of filled polymers. Counterclockwise from lower left: (a) Atomistic; (b) Coarse-grained MD; (c) Mesoscale continuum simulations; (d) finite element macroscale simulations.

calculations. The link between the MD simulations and the TDGL/CHC simulations was less direct, and made only qualitatively through incorporation of filler-polymer interaction terms in the CHC free energy functional that were attractive or neutral to one phase or the other. A closer link can be made by incorporating more details from the MD simulation, including e.g. composition- position-, and/or temperature-dependent mobility, and compressibility. Not discussed here are links yet to be made between our “coarse-grained” MD simulations and more atomistically accurate simulations of polymer-filler interactions, using, e.g. united atom or explicit atom force fields for the filler and polymers derived from quantum chemistry calculations.

## ACKNOWLEDGMENTS

We acknowledge useful discussions with E. Amis, P. Cummings, J. Douglas, E. Fuller, C. Han, A. Karim, J. Kieffer, B. Lee, A. Nakatani, N. Parekh, and T. Schröder.

## REFERENCES

1. G. Wypych, *Handbook of Fillers* (ChemTec Publishing, 1999).
2. M.C. Roco, S. Williams, and P. Alivisatos (Eds.), *Nanotechnology Research Directions: IWGN Workshop Report Vision for Nanotechnology in the Next Decade* (Kluwer Academic Publishers, 2000).
3. E.P. Giannelis, *Adv. Mater.* **8**, 29 (1996).
4. J.J. Schwab and J.D. Lichtenhan, *Appl. Organomet. Chem.* **12**, 707(1998).
5. F.J. Feher, D. Soulivong, A.G. Eklund, and K.D. Wyndham, *Chem. Commun.* **13**, 1185 (1997).
6. M.P. Allen and D.J. Tildesley, *Computer simulation of liquids* (Oxford, 1987).
7. F.W. Starr, T.B. Schröder, and S.C. Glotzer, cond-mat/0007486. (2000).
8. S.C. Glotzer, *Ann. Rev. in Comp. Phys.* **2**, 1 (1995).
9. B.P. Lee, J.F. Douglas, S.C. Glotzer, *Phys. Rev. E* **60**, 5812 (1999).
10. J.N. Reddy, *An introduction to the finite element method* (Mc-Graw-Hill, 1993).
11. S.C. Glotzer, C. Han, and E. Fuller, unpublished.
12. S.C. Glotzer and P.T. Cummings, unpublished.
13. E.K. Lin, R. Kolb, S.K. Satija, and W.L. Wu, *Macromolecules* **32**, 3753 (1999).
14. P. Cousin and P. Smith, *J. Poly. Sci. B: Poly. Phys.* **32**, 459. (1994).
15. G. Tsagaropoulos and A. Eisenberg, *Macromolecules* **28**, 6067 (1995).
16. N. Sombatsompop, *J. Appl. Poly. Sci.* **74**, 1129 (1999).
17. J.A. Forrest and R.A.L. Jones, in *Polymer surfaces, interfaces, and thin films*, eds. A. Karim and S. Kumar (World Scientific, 2000) pp. 251-294.
18. R.L. Jones, S.K. Kumar, D.L. Ho, R.M. Briber, and T.P. Russell, *Nature* **400**, 146 (2000).
19. J. Kraus, P. Müller-Buschbaum, T. Kuhlmann, D.W. Schubert, and M. Stamm, *Europhys. Lett.* **49**, 210 (2000).
20. S.K. Kumar, M. Vacatello, and D.Y. Yoon, *J. Chem. Phys.* **89**, 5206 (1989); *Macromolecules* **23**, 2189 (1990).
21. J.-S. Wang and K. Binder, *J. Phys. I France* **1**, 1583 (1991).
22. W.E. Wallace, J.H. van Zanten, W.L. Wu, *Phys. Rev. E* **52**, 3329 (1995).
23. J.H. van Zanten, W.E. Wallace, W.L. Wu, *Phys. Rev. E* **53**, 2053 (1996).

24. J.A. Forrest, K. Dalnoki-Veress, and J.R. Dutcher, *Phys. Rev. E* **56**, 5705 (1997).
25. J.A. Forrest, C. Svanberg, K. Revesz, M. Rodahl, L.M. Torell, B. Kasemo, *Phys. Rev. E* **58**, 1226 (1998).
26. S.H. Anastasiadis, K. Karatasos, G. Vlachos, E. Manias, and E.P.Giannelis, *Phys. Rev. Lett.* **84**, 915 (2000).
27. R.B. Bird, C.F. Curtiss, R.C. Armstrong, and O. Hassager, *Dynamics of Polymeric Liquids: Kinetic Theory, Vol. 2.* (John Wiley and Sons, 1987).
28. C. Bennemann, W. Paul, J. Baschnagel, and K. Binder, *J. Phys. Cond. Mat.* **11**, 2179 (1999).
29. C. Bennemann, C. Donati, J. Baschnagel, and S.C. Glotzer, *Nature* **399**, 246 (1999).
30. J.P. Hansen and I.R. McDonald, *Theory of Simple Liquids* (Academic Press, 1986).
31. P.G. Debenedetti, *Metastable Liquids* (Princeton Univ. Press 1996).
32. Confinement may play an additional role in  $T_g$  shifts in both filled polymers and ultra-thin films. The heterogeneous nature of the dynamics of polymer melts gives rise to a potentially large characteristic length scale near  $T_g$  [28,29,33,34]; thus confinement may shift  $T_g$  in a fashion similar to the way finite size shifts  $T_c$  in conventional critical phenomena; a study of this is underway.
33. S.C. Glotzer, *J. Non-Cryst. Solids* **274**, 342 (2000).
34. M.D. Ediger, *Ann. Rev. Phys. Chem.* (in press).
35. J.H. Gibbs, and E.A. DiMarzio, *J. Chem. Phys.* **28**, 373 (1958).
36. G. Adam and J.H. Gibbs, *J. Chem. Phys.* **43**, 139 (1965).
37. A. Scala, F.W. Starr, E. La Nave, F. Sciortino, and H.E. Stanley, *Nature* **406**, 166 (2000).
38. S. Sastry, *Phys. Rev. Lett.* **85**, 590 (2000).
39. F.W. Starr *et al.*, *Phys. Rev. E*, **63** in press (2001).
40. F. Varnik, J. Baschnagel, and K. Binder, *J. Phys. IV* **10**, 239 (2000).
41. J.A. Torres, P.F. Nealey, J.J. de Pablo, *Phys. Rev. Lett.* **85**, 3221 (2000).
42. J.W. Cahn, J.E. and Hilliard, *J. Chem. Phys.* **28**, 258 (1958).
43. J.W. Cahn, *Acta Metall.* **9**, 795 (1961); *ibid* **10**, 179 (1962); *J. Appl. Phys.* **34**, 3581 (1963).
44. S.C. Glotzer and A. Coniglio, *Phys. Rev. E* **50**, 4241 (1994).
45. S.C. Glotzer, E. DiMarzio, and M. Muthukumar, *Phys. Rev. Lett.* **74**, 2034 (1995).
46. J. Christensen, K. Elder, and H.C. Fogedby, *Phys. Rev. E* **54**, 2212 (1996).
47. M. Motoyama, *J. Phys. Soc. Japan* **65**, 1894. (1996).
48. S. Puri, H.L. Frisch, *J. Phys. A* **27**, 6027 (1994).
49. A.M. Lapena, S.C. Glotzer, S.A. Langer, and A.J. Liu, *Phys. Rev. E* **60**, 29 (1999).
50. N.M. Maurits, G.J.A. Sevink, A.V. Zvelindovsky, J.G.E.M. Fraaije, *Macromolecules* **32**, 7674 (1999).
51. V.V. Ginzburg, G. Peng, F. Qiu, and A.C. Balazs, *Phys. Rev. E* **60**, 4352 (1999).
52. R. Israels, *et al.*, *J. Chem. Phys.* **102**, 8149 (1995).
53. G.J.A. Sevink, A.V. Zvelindovsky, B.A.C. van Vlimmeren, N.M. Maurits, and J.G.E.M. Fraaije, *J. Chem. Phys.* **110**, 2250 (2000).
54. A. Karim, *et al.*, *Phys. Rev. E* **49**, 6273 (1998).
55. G.W. Peng, F. Qiu, V.V. Ginzburg, D. Jasnow, and A.C. Balazs, *Science* **288**, 1802 (2000).
56. F. Qiu, *et al.*, *Langmuir* **15**, 4952 (1999).
57. K.F. Freed, *J. Chem. Phys.* **105**, 10572 (1996).
58. P.K. Brazhnik, K.F. Freed, and H. Tang, *J. Chem. Phys.*, **101**, 9143 (1994).
59. D.L. Mills, *Phys. Rev. B* **3**, 3887 (1971).

60. K. Binder, in *Phase transitions and critical phenomena*, eds. C. Domb and J.L. Lebowitz, **8**, 1 (1983)..
61. A. Karim, J.F. Douglas, G. Nisato, D.-W. Liu, and E.J. Amis, *Macromolecules* **32**, 5917 (1999).
62. W.C. Carter, S.A. Langer, E. and Fuller, *The OOF Manual: Version 1.0*. (National Technical Information Service, 1998).
63. More information can be found at <http://www.ctcms.nist.gov/oof>.
64. N. Parekh, E. Fuller, C. Han, and S.C. Glotzer, (unpublished).